

Breast Cancer Staging in a Single Session: Whole-Body PET/CT Mammography

Till A. Heusner¹, Sherko Kuemmel², Lale Umutlu¹, Angela Koeninger², Lutz S. Freudenberg³, Elke A.M. Hauth¹, Klaus R. Kimmig², Michael Forsting¹, Andreas Bockisch³, and Gerald Antoch¹

¹Department of Diagnostic and Interventional Radiology and Neuroradiology, University Hospital Essen, University at Duisburg-Essen, Essen, Germany; ²Department of Gynecology and Obstetrics, University Hospital Essen, University at Duisburg-Essen, Essen, Germany; and ³Department of Nuclear Medicine, University Hospital Essen, University at Duisburg-Essen, Essen, Germany

Our objective was to compare the diagnostic accuracy of an all-in-one protocol of whole-body ¹⁸F-FDG PET/CT and integrated ¹⁸F-FDG PET/CT mammography with the diagnostic accuracy of a multimodality algorithm for initial breast cancer staging.

Methods: Forty women (mean age, 58.3 y; range, 30.8–78.4 y; SD, 12 y) with suspected breast cancer were included. For the primary tumor, we compared ¹⁸F-FDG PET/CT mammography versus MRI mammography; for axillary lymph node status, ¹⁸F-FDG PET/CT versus clinical investigation and ultrasound; and for distant metastases, ¹⁸F-FDG PET/CT versus a multimodality staging algorithm. Histopathology and clinical follow-up served as the standard of reference. The Fisher exact test evaluated the significance of differences ($P < 0.05$). Alterations in patient management caused by ¹⁸F-FDG PET/CT were documented.

Results: No significant differences were found in the detection rate of breast cancer lesions (¹⁸F-FDG PET/CT, 95%; MRI, 100%; $P = 1$). ¹⁸F-FDG PET/CT correctly classified lesion focality significantly more often than did MRI (¹⁸F-FDG PET/CT, 79%; MRI, 73%; $P < 0.001$). MRI correctly defined the T stage significantly more often than did ¹⁸F-FDG PET/CT (MRI, 77%; ¹⁸F-FDG PET/CT, 54%; $P = 0.001$). ¹⁸F-FDG PET/CT detected axillary lymph node metastases in 80% of cases; clinical investigation/ultrasound, in 70%. This difference was not statistically significant ($P = 0.067$). Distant metastases were detected with ¹⁸F-FDG PET/CT in 100% of cases, and the multimodality algorithm identified distant metastases in 70%. This difference was not statistically significant ($P = 1$). Three patients had extraaxillary lymph node metastases that were detected only by PET/CT (cervical, retroperitoneal, mediastinal/internal mammary group). ¹⁸F-FDG PET/CT changed patient management in 12.5% of cases. **Conclusion:** Our data suggest that a whole-body ¹⁸F-FDG PET/CT mammography protocol may be used for staging breast cancer in a single session. This initial assessment of the ¹⁸F-FDG PET/CT protocol indicates similar accuracy to MRI for the detection of breast cancer lesions. Although MRI seems to be more accurate when assessing the T stage of the tumor, ¹⁸F-FDG PET/CT seems able to more accurately define lesion focality. Although ¹⁸F-FDG PET/CT mammography was able to detect axillary lymph node metastases with a high sensitivity, this method cannot soon be ex-

pected to replace the combination of clinical examination, ultrasound, and sentinel lymph node biopsy for axillary assessment.

Key Words: breast cancer; oncology; PET/CT; whole-body imaging; mammography

J Nucl Med 2008; 49:1215–1222

DOI: 10.2967/jnumed.108.052050

Breast cancer, the most common type of cancer and the second leading cause of cancer-related death in women in western countries (1), involves not only the elderly but also many younger patients (2). Once breast cancer is diagnosed, the tumor stage must be accurately determined before therapy can be chosen and the prognosis can be known (3). So far, initial breast cancer staging has been based on a multimodality approach: x-ray mammography is the most widely used technique for diagnosis of the primary lesion in both symptomatic and asymptomatic patients (4,5). Correlation of mammography findings with breast ultrasound and MRI has been helpful for differential diagnosis of a breast lesion and for detection of occult breast tumors (6–8). Staging of the primary tumor by these imaging modalities is complemented by staging for locoregional lymph node metastases and distant metastases with methods including sentinel lymph node biopsy, chest radiography, axillary and abdominal ultrasound, and bone scintigraphy. This multimodality approach, however, is time consuming. Additionally, sentinel lymph node biopsy is invasive and carries a risk of periprocedural complications. Thus, a noninvasive, single-session approach to breast cancer staging may be desirable.

¹⁸F-FDG PET/CT accurately stages various types of tumors (9–11). In addition, whole-body ¹⁸F-FDG PET/CT is beneficial for staging breast cancer (12–14) and for monitoring therapy in breast cancer patients (15). However, ¹⁸F-FDG PET/CT has predominantly been used to detect distant metastases in breast cancer patients. Mammography in conjunction with ultrasound and MRI mammography has remained the method of choice for imaging the primary tumor, and ultrasound of the axillary fossa and sentinel

Received Mar. 2, 2008; revision accepted Apr. 14, 2008.

For correspondence or reprints contact: Gerald Antoch, Department of Diagnostic and Interventional Radiology and Neuroradiology, University Hospital Essen, University at Duisburg-Essen, Essen, Germany.

E-mail: gerald.antoch@uni-duisburg-essen.de

COPYRIGHT © 2008 by the Society of Nuclear Medicine, Inc.

lymph node biopsy have remained the methods of choice for detecting potential locoregional lymph node metastases.

Recently, the technical feasibility of a dedicated whole-body ¹⁸F-FDG PET/CT protocol with integrated ¹⁸F-FDG PET/CT mammography was reported, and this protocol has been implemented in clinical routine (16). However, the diagnostic accuracy of this 1-step staging algorithm has not yet been defined. Thus, the aim of this study was to assess the accuracy of whole-body ¹⁸F-FDG PET/CT mammography for breast cancer staging, compared with an established staging algorithm that is currently recommended by German staging guidelines (17).

MATERIALS AND METHODS

Patients

Forty women (mean age, 58.3 y; range, 30.8–78.4 y; SD, 12 y) with suspected malignancy on conventional x-ray mammography (performed either for screening or because of a clinically suggestive, palpable mammary mass) were referred for supine whole-body ¹⁸F-FDG PET/CT with integrated prone ¹⁸F-FDG PET/CT mammography. In addition, all patients underwent further staging procedures recommended by the guidelines, including MRI mammography (mean interval between MRI mammography and ¹⁸F-FDG PET/CT mammography, 1 d; range, 0–10 d; SD, 2.2 d), ultrasound of the axilla, sentinel lymph node scintigraphy followed by sentinel lymph node biopsy (mean interval between sentinel lymph node biopsy/axillary dissection and ¹⁸F-FDG PET/CT, 11 d; range, 2–26 d; SD, 6.23 d), bone scintigraphy, chest radiography, and ultrasound of the abdomen. If the axilla was clinically suspected to harbor lymph node metastases, no sentinel lymph node biopsy was performed and the patient went directly to surgery. All patients signed a consent form that detailed the use of intravenous ¹⁸F-FDG, CT contrast material, and MRI contrast material and rare potential side effects. This was a retrospective study performed in accordance with the regulations of the local ethics committee.

Whole-Body PET/CT Mammography

Dual-modality whole-body ¹⁸F-FDG PET/CT scans were obtained on a Biograph PET/CT system (Siemens Molecular Imaging).

The system provides separate CT and PET datasets, which can be accurately fused on a computer workstation. Patients fasted for at least 6 h before receiving an intravenous dose of ¹⁸F-FDG (mean, 274 MBq; range, 210–370 MBq). Before injection of the tracer, a blood sample was taken to ensure that blood glucose levels were within the reference range. Patients with a level exceeding 150 mg/dL were not included in the study. A water-based oral contrast agent (1,500 mL) was administered within the ¹⁸F-FDG uptake time to mark the bowel (18).

¹⁸F-FDG PET/CT was performed approximately 60 min after intravenous administration of ¹⁸F-FDG. The dedicated whole-body ¹⁸F-FDG PET/CT mammography protocol was divided into 2 parts. First, whole-body ¹⁸F-FDG PET/CT from the head to the upper thighs was performed with the patient supine. CT images were acquired in the caudocranial direction with 100 mA/s at 130 kV. An iodinated contrast agent (140 mL, Ultravist 300; Schering AG) containing 300 mg of iodine per milliliter was administered with an automated injector (XD 5500; Ulrich Medical Systems) using a biphasic technique with a flow rate of 3 mL/s for the first 90 mL and 1.5 mL/s for the next 50 mL. The start delay was set to 50 s. All images were reconstructed with a 5-mm slice thickness and a 2.4-mm increment. A limited breath-hold technique was used to avoid motion-induced artifacts near the diaphragm (19). After acquisition of the CT data, PET images were obtained in 3-dimensional mode. The PET emission time for the whole-body scan was adapted to the patients' body weight: patients weighing less than 65 kg were scanned for 4 min per bed position; patients weighing 65–85 kg, 5 min per bed position; and patients weighing more than 85 kg, 6 min per bed position. Iterative algorithms (Fourier rebinning and attenuation-weighted ordered-subsets expectation maximization, nonlinear) with 2 iterations and 8 subsets were used for image reconstruction. Data were filtered (full width at half maximum, 5.0 mm) and corrected for scatter.

The second part of the imaging protocol was performed after repositioning the patient prone, using a special breast-positioning aid (Mamma Comfort; Additec GmbH, Fig. 1) that allowed a pendant breast position similar to that for the MRI breast coil used in clinical routine. In accord with the method of Kumar et al. (20), the prone PET acquisition started approximately 110 min after the ¹⁸F-FDG injection. A lateral topogram was obtained to define the scan range from the axillary fossa to the lower end of the breasts.

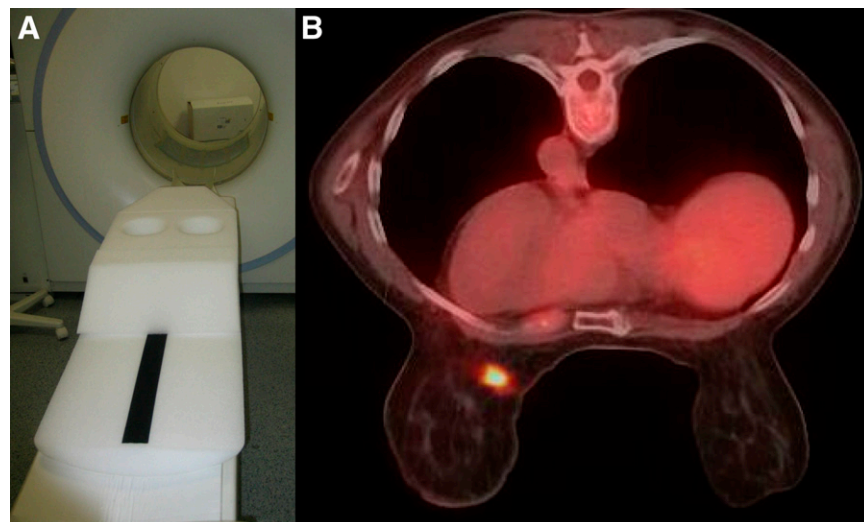


FIGURE 1. (A) Positioning device for prone ¹⁸F-FDG PET/CT mammography, the Mamma Comfort Board (Additec GmbH), made from foam plastic. (B) Transverse ¹⁸F-FDG PET/CT mammogram of ¹⁸F-FDG PET-positive breast cancer lesion.

Again, CT was performed first, followed by PET. No additional contrast medium was applied for prone PET/CT. Images were acquired in the caudocranial direction. The CT parameters were the same as for the supine scan. The number of PET bed positions depended on the size of the field of view from the axilla to the lower end of the breasts. The PET emission time ranged from 6 to 10 min, depending on the volume of the breast (A cup, 6 min; B cup, 7 min; C cup, 8 min; D cup, 9 min; larger than D cup, 10 min). PET image reconstruction was performed according to the supine protocol.

MRI Mammography

All patients underwent MRI mammography. Dynamic contrast-enhanced breast MRI was performed on a 1.5-T MRI scanner with multichannel capability (Magnetom Espree; Siemens Medical Solutions). A standard 8-channel phased-array breast coil (Siemens Medical Solutions) was used. Patients were positioned prone. A localizer sequence was obtained. An axial T2-weighted turbo spin-echo sequence was obtained (6.18 min; repetition time/echo time, 7,000/95; flip angle, 180°; field of view, 37 cm; slice thickness, 2 mm; no gap; number of excitations, 3; matrix, 384 × 384). Then, a dynamic axial T1-weighted 3-dimensional fast low-angle shot sequence was obtained (11.59 min; repetition time/echo time, 11/4.76; flip angle, 15°; field of view, 37 cm; slice thickness, 2 mm; gap, 0.4-mm; number of excitations, 1; matrix, 365 × 384). This was followed by intravenous injection (Solaris power injector; Spectris) of gadopentetate dimeglumine (Magnevist; Schering) at a concentration of 0.1 mmol/kg of body weight followed by a 20-mL saline flush. The flow rate was 2 mL/s. After the dynamic series, the contrast-enhanced images were subtracted from the unenhanced images.

Image Analysis

The ^{18}F -FDG PET/CT data were analyzed by 2 radiologists (5 and 3 y of PET/CT experience) and a nuclear medicine specialist (5 y of PET/CT experience). Diagnoses were made in consensus. All images were evaluated on an AW Suite 5.5.3e Volume Viewer Plus Workstation (GE Healthcare) connected to a PACS workstation (GE Healthcare). ^{18}F -FDG PET/CT scans were reviewed in 3 orthogonal planes (axial, coronal, and sagittal). PET scans were also evaluated in the non-attenuation-corrected mode. MRI scans were evaluated by 2 radiologists in consensus (5 and 3 y of MRI mammography experience). A PACS workstation was used for image evaluation.

Evaluation of Breast. On PET/CT, a breast lesion was suspected to be malignant if it showed increased contrast enhancement, compared with the surrounding tissue (attenuation measurements with regions of interest and expressed in Hounsfield units). Suspicion was confirmed by elevated tracer uptake, compared with the adjacent breast tissue. Quantitative analysis of PET was performed, with the maximal standardized uptake value (SUVmax) of the suggestive lesion corrected for body weight.

On MRI, breast lesions were rated according to the American College of Radiology Breast Imaging Reporting and Data System lexicon (21). Abnormal enhancement was characterized as a mass or nonmass lesion. Both the morphologic appearance (size, shape, and pattern of enhancement) and the temporal enhancement pattern were evaluated. Time-signal-intensity curves (progressive, plateau, or washout) were generated for all enhancing lesions. Additionally a 3-time-point analysis was performed using the

3-time-point software package (CAD Sciences) as described in the literature (22–25).

Findings rated as malignant with MRI or ^{18}F -FDG PET/CT were classified as unifocal lesions (single lesion in 1 quadrant), multifocal lesions (more than 1 lesion in the same quadrant), or multicentric lesions (more than 1 quadrant affected by breast cancer lesions, or distance between breast cancer lesions more than 4 cm within 1 quadrant).

Evaluation of Axillary Fossa. The ipsilateral axillary fossa was assessed for potential lymph node metastases with ^{18}F -FDG PET/CT. With ^{18}F -FDG PET/CT, axillary lymph node assessment was based on both size and metabolic activity. Glucose uptake with an SUVmax higher than 2.5 indicated malignancy (26), independent of lymph node size. A cross-sectional diameter of more than 10 mm and a loss of fatty hilum supported the diagnosis of a lymph node metastasis. Central necrosis of a lymph node on CT was considered malignant independent of the PET data.

Distant Metastases. In addition, ^{18}F -FDG PET/CT datasets were assessed for distant metastases. Assessment of distant metastases was based on quantitative and qualitative analyses. ^{18}F -FDG PET/CT data were evaluated qualitatively for regions of focally increased glucose metabolism and quantitatively by SUVmax measurements. Glucose uptake qualitatively higher than in the surrounding tissue and a SUVmax higher than 2.5 indicated malignancy (26).

Data Analysis

Primary Tumor. The sensitivity for detection of malignant breast cancer lesions with ^{18}F -FDG PET/CT and MRI was calculated. The SUVmax of breast cancer lesions, categorized by histopathologic entity, was determined. In addition, the ability of both imaging procedures to accurately differentiate unifocal, multifocal, and multicentric lesions was determined. The T stage was assessed with ^{18}F -FDG PET/CT and MRI on the basis of morphology (lesion size and contrast enhancement) and compared between imaging procedures. Specificities were not calculated, because all the included patients had known breast cancer.

Ipsilateral Axilla. The sensitivity of ^{18}F -FDG PET/CT for the detection of axillary lymph node metastases was calculated and compared with the combined clinical examination and ultrasound results. The SUVmax and the square diameter of axillary lymph nodes positive on ^{18}F -FDG PET/CT but negative on clinical examination and ultrasound were determined. The SUVmax of axillary lymph nodes true-positive and false-negative on ^{18}F -FDG PET/CT was determined.

Distant Metastases. The sensitivity of ^{18}F -FDG PET/CT for the detection of distant metastases was assessed and compared with the results of the recommended multimodality staging algorithm, including abdominal ultrasound, chest radiography, and bone scintigraphy.

Extraaxillary Lymph Node Metastases. Extraaxillary lymph node metastases were documented.

Changes in Patient Management. Potential alterations in the patients' management based on previously unknown findings on ^{18}F -FDG PET/CT were documented.

Standard of Reference. Histopathologic evaluation of tumor biopsy samples ($n = 14$, performed within a mean of 8 d from the day of PET/CT; range, 1–22 d; SD, 4 d) or resected breast tumors ($n = 28$) served as the standard of reference for the primary lesion. Evaluation of T stage was limited to the 28 patients who underwent tumor resection. The remaining 12 patients were treated

TABLE 1
T Stages of Resected Breast Cancers and Numbers of Patients Correctly Staged with PET/CT Mammography and MRI Mammography

T stage	Gold standard <i>n</i>	Correctly staged with PET/CT		Correctly staged with MRI mammography	
		<i>n</i>	%	<i>n</i>	%
T1a	0	—	—	—	—
T1b	4	2	50	4	100
T1c	11	8	72	9	82
T2	11	3	27	7	64
T3	2	2	100	2	100
T4	0	—	—	—	—

systemically in either a neoadjuvant setting ($n = 7$) or a palliative setting ($n = 5$). Histopathologic evaluation of the resected sentinel lymph node or resected axillary lymph nodes, as well as clinical follow-up (mean, 155 d; range, 31–1,406 d; SD, 206 d), served as the standard of reference for axillary lymph node stage. Histopathologic results or clinical follow-up served as the standard of reference for potential distant metastases.

Statistical Analysis

For the primary tumor, ^{18}F -FDG PET/CT mammography was compared with MRI mammography for the detection of breast cancer lesions, the correct T stage, and the correct classification of breast lesion focality. In addition, the SUVmax of breast cancer lesions subdivided by histopathologic entities (infiltrating ductal, infiltrating lobular, mixed ductal/lobular, mucinous, anaplastic, tubular carcinoma, and adenocarcinoma) was compared for statistically significant differences.

For N stage, ^{18}F -FDG PET/CT was compared with a combination of clinical examination and ultrasound.

TABLE 2
Histopathology and SUVmax of Breast Cancers

Histopathology	<i>n</i>	%	SUVmax		
			Mean	Range	SD
Infiltrating ductal	20	47	4.6	0.8–11.7	3.3
Infiltrating lobular	11	26	2.9	0.8–5.9	1.6
Mixed ductal/lobular	4	9	5.6	2–10.5	3.7
Mucinous	3	7	3.1	2.1–4.9	1.5
Anaplastic	2	5	—	2.9–11.4	—
Tubular	1	2	—	1.6	—
Adenocarcinoma	1	2	—	2.3	—
Total	42	100	4.2	0.8–11.7	3.1

For M stage, ^{18}F -FDG PET/CT was compared with a conventional staging algorithm, including abdominal ultrasound, chest radiography, and bone scintigraphy.

All differences between imaging modalities were tested for potential statistical significance with the Fisher exact test. The SUVmax of the breast cancer lesions, categorized by histopathologic entity, was tested for significance with the Mann–Whitney test. A *P* value of less than 0.05 indicated a significant difference.

RESULTS

Primary Tumor

The 40 patients had 42 histopathologically verified breast cancer lesions. Thirty-eight patients had unilateral disease, and 2 patients bilateral. Table 1 summarizes T stage, and Table 2 histopathologic type. Differences in the SUVmax of different histologic types were not statistically significant ($P > 0.05$).

The sensitivity for the detection of breast cancer lesions was 95% with ^{18}F -FDG PET/CT. Two breast cancer lesions were not detectable with ^{18}F -FDG PET/CT. These were

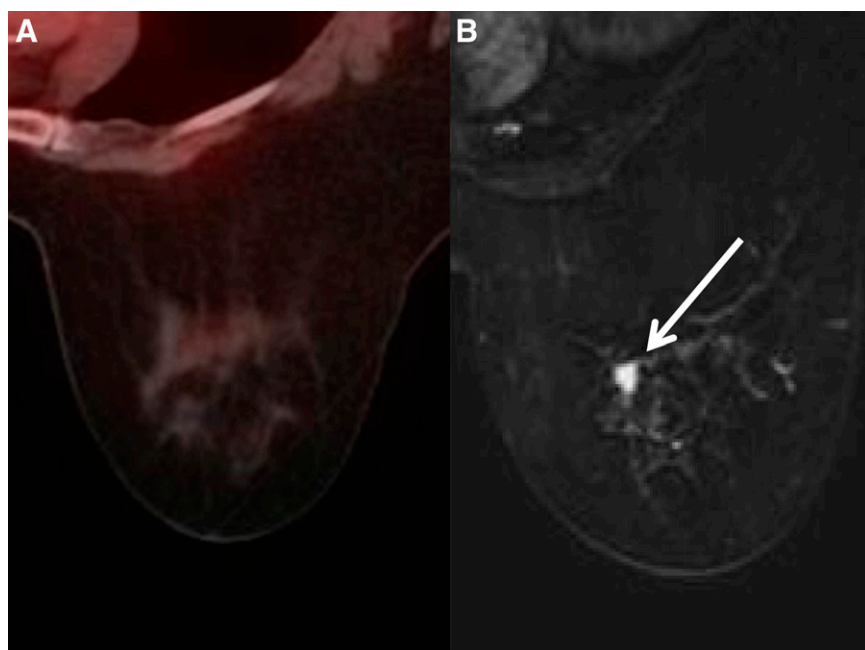


FIGURE 2. Unifocal primary breast cancer in inner lower quadrant of left breast in 76-y-old woman. (A) Lesion was not detected by ^{18}F -FDG PET/CT (A). (B) MRI mammography identified lesion correctly (arrow).

TABLE 3

Number of Solitary, Multifocal, and Multicentric Breast Cancer Lesions According to Standard of Reference

Histopathologic pattern	<i>n</i>	%
Solitary	15	46
Multifocal	6	18
Multicentric	12	36
Total	33	100

T1b and T2 infiltrating lobular breast cancer (Fig. 2). MRI detected 100% of the breast cancer lesions. The difference was not statistically significant ($P = 1$). However, there was a statistically significant difference when assessing the T stage of breast cancer. MRI classified the T stage correctly in 77% of cases; ^{18}F -FDG PET/CT, in 54% of cases ($P = 0.001$).

For 33 of the 42 lesions, histopathologic findings differentiating between solitary, multifocal, and multicentric lesions were available (Table 3). In 9 lesions, the pathologist could make no conclusion on focality (only biopsy findings were available, and patients were treated either neoadjuvantly or palliatively). Of these 33 lesions, 2 were ^{18}F -FDG PET/CT-negative. ^{18}F -FDG PET/CT was able to classify the focality pattern correctly in 26 of the 33 ^{18}F -FDG PET/CT-positive lesions (79%). MRI was able to classify the focality pattern correctly in 24 of 33 MRI-visible lesions (73%) (Fig. 3). The difference was statistically significant ($P < 0.001$).

Ipsilateral Axilla

In all patients, a clinical examination and ultrasound were performed. In 30 patients, either a sentinel lymph node biopsy or an axillary lymph node dissection was performed.

Ten of the 30 patients had histopathologically proven axillary lymph node metastases. ^{18}F -FDG PET/CT detected axillary metastatic spread in 8 of 10 patients (80%). The combination of clinical investigation and axillary ultrasound detected axillary metastatic spread in 7 of 10 patients (70%). This difference was not statistically significant ($P = 0.067$). ^{18}F -FDG PET/CT detected an axillary lymph node metastasis that was positive on PET but falsely negative on clinical investigation and axillary ultrasound. The SUVmax of this metastasis was 4.6, and the square diameter was 6 mm. The mean SUVmax of true-positive axillary lymph nodes was 9.1 (range, 2.6–15.8; SD, 5.8), the mean SUVmax of false-negative lymph nodes was 1.4 (range, 0.9–1.9; SD, 0.7). In 10 patients, neither a sentinel lymph node biopsy nor an axillary lymph node dissection was performed after ^{18}F -FDG PET/CT, as the therapeutic objectives were either neoadjuvant or palliative.

Extraaxillary Lymph Node Metastases

In 3 patients, breast cancer metastases to lymph nodes were positive on ^{18}F -FDG PET but were missed by the conventional staging algorithm. In the first patient, the metastasis was adjacent to the left internal jugular vein; in the second, it was retroperitoneal; and in the third, one metastasis was adjacent to the ipsilateral internal mammary artery and another was mediastinal.

Distant Metastases

In 30 patients, no distant metastases were found. In 10 patients, distant metastases were found. ^{18}F -FDG PET/CT detected the distant metastases in all 10 of these patients. The staging algorithm recommended according to current guidelines revealed 7 of the 10 patients with distant metastases (70%). Thus, compared with the conventional staging

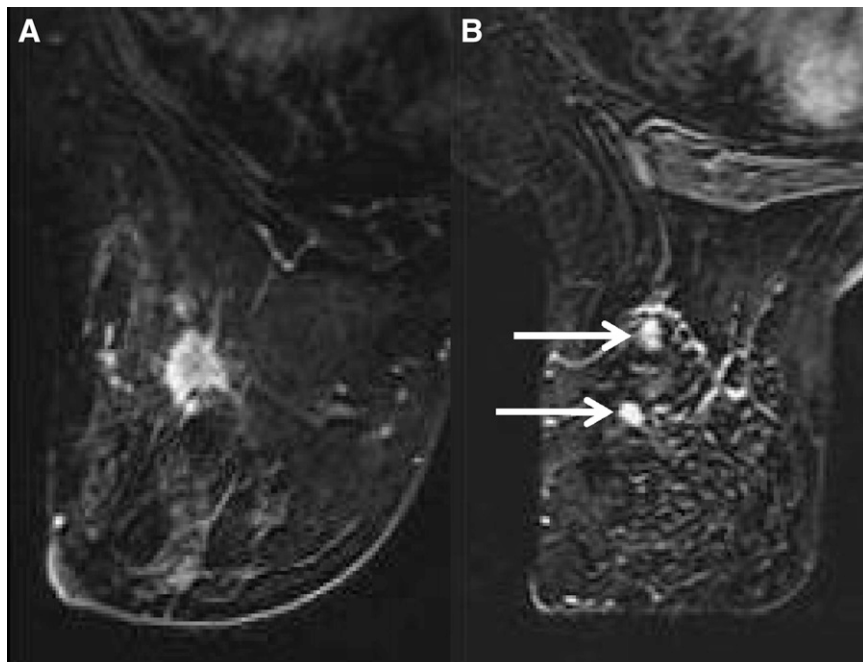


FIGURE 3. (A) Unifocal breast cancer lesion detected by MRI. (B) Two additional lesions (arrows) were detected in different quadrant of same breast and were histologically proven to be benign. MRI falsely rated this disease as multifocal. ^{18}F -FDG PET/CT correctly rated lesion as solitary.



FIGURE 4. Clinically occult cervical lymph node metastasis detected only by ^{18}F -FDG PET/CT, based on elevated ^{18}F -FDG uptake (SUV_{max}, 3.1). On clinical investigation and ultrasonography, this lymph node, with square diameter of 6 mm, was not suspected of harboring malignancy.

algorithm, ^{18}F -FDG PET/CT changed the M stage from M0 to M1 in 3 patients. The difference was not statistically significant ($P = 1$).

Alteration of Patient Management

^{18}F -FDG PET/CT influenced further therapeutic decisions in 5 patients (12.5%). In 3 patients, ^{18}F -FDG PET/CT altered the M stage from M0 to M1; in 1 of these patients, a clinically occult lymph node metastasis adjacent to the internal jugular vein was diagnosed with ^{18}F -FDG PET/CT and surgically resected (Fig. 4; standard of reference, histopathology). In another patient, a pulmonary metastasis (not detected on chest radiography; Fig. 5) was detected. The therapeutic objective changed from local treatment to systemic endocrinologic therapy (standard of reference, follow-up). In 1 patient, an osteolytic bone metastasis (not detectable with bone scintigraphy; Fig. 6; standard of reference, histopathology) was detected and surgically resected. In 2 patients, synchronous tumors and clinically occult lymph node metastases were diagnosed: the first patient had colon cancer (Fig. 7; standard of reference, histopathology) and clinically occult lymph node metastases (mediastinal and internal mammary group; Fig. 7; standard of reference, histopathology and mediastinoscopy). The colon cancer was resected. Additionally, systemic therapy with an aromatase inhibitor was started. The second patient had an infracarinal lymph node metastasis (standard of reference, follow-up) of bronchial carcinoma that had been treated before. The patient was treated with chemotherapy.

DISCUSSION

^{18}F -FDG PET/CT, as a noninvasive, all-in-one imaging modality, has been reported to be useful in whole-body staging, restaging, and monitoring of treatment response in breast cancer patients (12,27,28). However, ^{18}F -FDG PET/CT has been used mainly for the evaluation of potential distant metastases. Its impact on the assessment of primary breast lesions and the axilla for lymph node metastases has not been assessed in larger cohorts. In a preliminary study, we investigated a dedicated ^{18}F -FDG PET/CT protocol for breast cancer staging (16). This protocol included supine whole-body ^{18}F -FDG PET/CT for tumor staging and integrated prone ^{18}F -FDG PET/CT mammography for the assessment of T stage and N stage. Although the technical feasibility of the protocol could be verified in a small patient population, data on the actual accuracy of such an all-in-one approach are still lacking. The data of the current study suggest that this ^{18}F -FDG PET/CT protocol may have similar sensitivity to MRI for the detection of intramammary cancer lesions. The results concerning tumor detection are in contrast to a report by Avril et al. (29), who found a sensitivity of only 25% for the detection of T1b breast carcinomas when assessed with PET alone. ^{18}F -FDG PET/CT detected 75% of these small carcinomas in the current analysis. We consider there to be 2 possible reasons for the higher sensitivity in the detection of breast cancer lesions in this analysis: the first reason may be the combination of CT with PET. The limited spatial resolution of PET may compromise detection of small tumors within the breasts, even when a dedicated positioning device is used. Adding contrast-enhanced CT to PET can reveal small contrast-enhancing breast lesions, as was found by Boone et al. Their study showed that the use of intravenous contrast material dramatically enhanced the visualization of breast tumor lesions on CT mammography (30). The second reason may be the time point at which PET was acquired: Avril (29) acquired PET scans 40–60 min after ^{18}F -FDG injection. In accord with Kumar (20) and Mavi (31), who documented a significant increase in the SUV_{max} of breast cancer lesions over time, we acquired the first PET scan approximately 60 min after tracer injection and the dedicated PET/CT scan of the breast approximately 110 min after injection. Both PET images were used for evaluating breast cancer lesions.

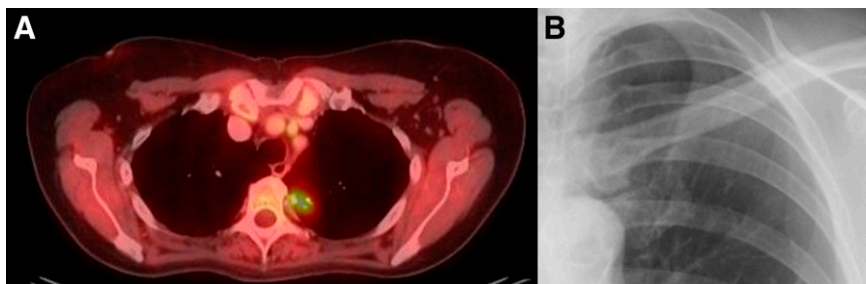


FIGURE 5. (A) Histopathologically proven pulmonary metastasis detected only by ^{18}F -FDG PET/CT. (B) Lesion was not detected by chest radiography and was the only distant metastasis in this 74-y-old patient.

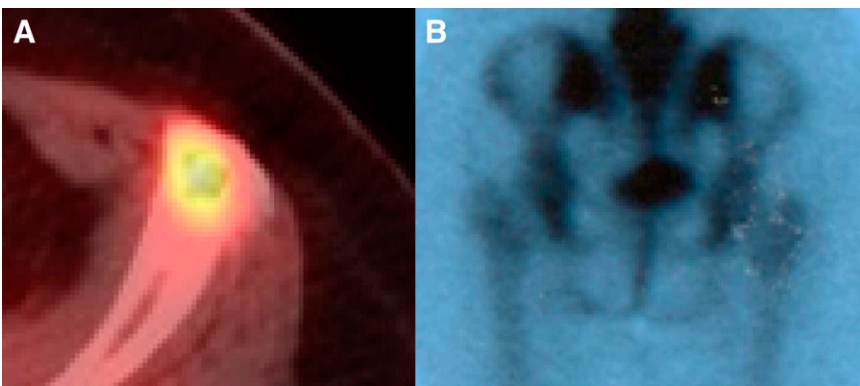


FIGURE 6. (A) Histologically proven osteolytic metastasis detected by ^{18}F -FDG PET/CT in left iliac bone. (B) On bone scintigraphy, lesion was called equivocal. This lesion was the only distant metastasis in this 62-y-old patient.

The reported data further indicate that ^{18}F -FDG PET/CT mammography may be more accurate than MRI mammography in pretherapeutically differentiating breast lesions as unifocal, multifocal, or multicentric. MRI has been known to be a sensitive but less specific modality when it comes to detection and characterization of breast cancer lesions (32–35). Six cases were falsely rated as multicentric with MRI in the current study. These were lesions that, with contrast enhancement, were classified as malignant but later proved to be benign on histopathology. In the planning of surgical therapy, differentiation of unifocal from multifocal and multicentric lesions is indispensable as it influences the decision on whether to surgically ablate the breast or perform breast-preserving surgery: although unifocal and multifocal lesions may be treated with excision, multicentric breast cancers require mamma ablation. Avril et al. reported that only 50% of multicentric or multifocal breast cancer sites were correctly identified by PET alone (36). In the current study, combined ^{18}F -FDG PET/CT offered correct classification in 84% of cases. This improvement over PET alone may also be attributed to the additional morphologic data and the later time point of the PET acquisition.

Presumably because of its excellent soft-tissue contrast, MRI was able to correctly predict the T stage in significantly more patients than ^{18}F -FDG PET/CT did. With CT as part of the ^{18}F -FDG PET scan, tumor margins are more difficult to determine than with MRI, especially in dense breast tissue. T staging seems to be a limitation of ^{18}F -FDG PET/CT mammography, when compared with MRI.

Compared with a conventional staging algorithm as recommended by the German Association of Gynaecology

and Obstetrics (17), whole-body ^{18}F -FDG PET/CT mammography was able to detect more distant metastases, with an impact on patient management in 12.5% of patients. Although these results seem intriguing, we acknowledge that, based on only 10 patients with distant metastases, this difference was not statistically significant. Again, a larger patient cohort will be required to further analyze these findings.

A lesion was called a metastasis on PET/CT if ^{18}F -FDG uptake was higher than in the surrounding tissue on qualitative analysis, with an SUV_{max} of more than 2.5 supporting the diagnosis. Fixed standardized uptake values have been discussed controversially in the literature, as inflammatory as well as physiologic processes may elevate the SUV_{max} to levels above 2.5. However, we believe in a combination of qualitative and quantitative assessment of PET/CT datasets, taking into account that false-positive results occur. The relatively few breast cancer lesions smaller than 1 cm may be considered another limitation of the study.

Before this study, only a few published studies had evaluated ^{18}F -FDG PET/CT for axillary lymph node staging. Wang et al. (37) reported a sensitivity of 80%, a specificity of 90%, and an accuracy of 87% in 15 patients with breast cancer. Yang et al. found a sensitivity of 88% for the detection of axillary lymph node metastases in patients with inflammatory breast cancer (38). Our data are comparable to these results and suggest that ^{18}F -FDG PET/CT is able to detect axillary lymph node metastases with a high sensitivity. However, the accuracy of the combination of clinical examination, axillary ultrasound examination, and additional sentinel lymph node tracking/sentinel lymph node

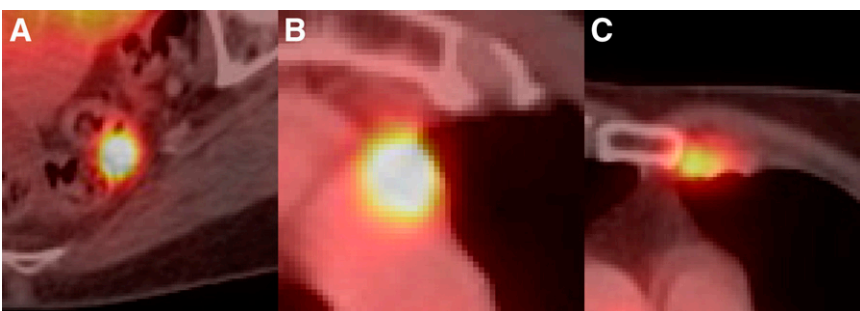


FIGURE 7. Clinically occult findings diagnosed only on ^{18}F -FDG PET/CT: carcinoma of sigmoid colon (A), mediastinal lymph node metastasis (B), and lymph node metastasis of internal mammary group (C) in 64-y-old patient.

biopsy will be higher than that of PET/CT because of the histopathologic information. The known limitations of both PET and CT for the detection of small metastases make it unlikely that the combination of the 2 modalities will soon replace the conventional axillary staging algorithm (including sentinel lymph node biopsy) (11).

CONCLUSION

Our data suggest that a whole-body ¹⁸F-FDG PET/CT mammography protocol may be used for staging breast cancer patients in a single session. This initial assessment of the ¹⁸F-FDG PET/CT protocol indicates similar accuracy to MRI for the detection of breast cancer lesions. MRI seems to more accurately assess T stage, but ¹⁸F-FDG PET/CT seems to more accurately define lesion focality. Although ¹⁸F-FDG PET/CT mammography was able to detect axillary lymph node metastases with a high sensitivity, it cannot be expected to soon replace the combination of clinical examination, ultrasound, and sentinel lymph node biopsy for axillary assessment. However, compared with a conventional staging algorithm, ¹⁸F-FDG PET/CT mammography was able to change patient management in a substantial number of patients. In the future, whole-body ¹⁸F-FDG PET/CT mammography may play an important role as an adjunct to MRI mammography and sentinel lymph node biopsy in high-risk patients, simultaneously providing an accurate assessment of lesion focality and whole-body tumor staging.

ACKNOWLEDGMENTS

We thank Alexander Stahl and Claudia Rehme for their expertise and critical comments. We gratefully acknowledge the efforts of our PET/CT and MRI staff. We thank Additec GmbH for providing the breast-positioning device.

REFERENCES

- Jemal A, Siegel R, Ward E, et al. Cancer statistics, 2006. *CA Cancer J Clin*. 2006;56:106–130.
- Smigal C, Jemal A, Ward E, et al. Trends in breast cancer by race and ethnicity: update 2006. *CA Cancer J Clin*. 2006;56:168–183.
- Thurlimann B, Muller A, Senn HJ. Management of primary breast cancer: an update. *Onkologie*. 2004;27:175–179.
- Agnese DM. Advances in breast imaging. *Surg Technol Int*. 2005;14:51–56.
- Scheidhauer K, Walter C, Seemann MD. FDG PET and other imaging modalities in the primary diagnosis of suspicious breast lesions. *Eur J Nucl Med Mol Imaging*. 2004;31(suppl 1):S70–S79.
- Rausch DR, Hendrick RE. How to optimize clinical breast MR imaging practices and techniques on your 1.5-T system. *Radiographics*. 2006;26:1469–1484.
- Berg WA, Gutierrez L, NessAiver MS, et al. Diagnostic accuracy of mammography, clinical examination, US, and MR imaging in preoperative assessment of breast cancer. *Radiology*. 2004;233:830–849.
- Winnekendonk G, Krug B, Warm M, Gohring UJ, Mallmann P, Lackner K. *Rofo*. 2004;176:688–693.
- Antoch G, Vogt FM, Freudenberg LS, et al. Whole-body dual-modality PET/CT and whole-body MRI for tumor staging in oncology. *JAMA*. 2003;290:3199–3206.
- Czernin J, Allen-Auerbach M, Schelbert HR. Improvements in cancer staging with PET/CT: literature-based evidence as of September 2006. *J Nucl Med*. 2007;48(suppl 1):78S–88S.
- Blodgett TM, Meltzer CC, Townsend DW. PET/CT: form and function. *Radiology*. 2007;242:360–385.
- Zangheri B, Messa C, Picchio M, Gianolli L, Landoni C, Fazio F. PET/CT and breast cancer. *Eur J Nucl Med Mol Imaging*. 2004;31(suppl 1):S135–S142.
- Tatsumi M, Cohade C, Mourtzikos KA, Fishman EK, Wahl RL. Initial experience with FDG-PET/CT in the evaluation of breast cancer. *Eur J Nucl Med Mol Imaging*. 2006;33:254–262.
- Radan L, Ben-Haim S, Bar-Shalom R, Guralnik L, Israel O. The role of FDG-PET/CT in suspected recurrence of breast cancer. *Cancer*. 2006;107:2545–2551.
- Beresford M, Lyburn I, Sanghera B, Makris A, Wong WL. Serial integrated ¹⁸F-fluorodeoxythymidine PET/CT monitoring neoadjuvant chemotherapeutic response in invasive ductal carcinoma. *Breast J*. 2007;13:424–425.
- Heusner T, Freudenberg LS, Kuehl H, et al. Whole-body PET/CT-mammography for staging breast cancer: initial results. *Br J Radiol*. May 28, 2008 [Epub ahead of print.]
- Kreienberg R, Kopp I, Lorenz W, et al. Diagnostik, therapie und nachsorge des mammakarzinoms der frau. In: *Leitlinien der Deutschen Krebsgesellschaft*. Frankfurt/Main, Germany: Informationszentrum für Standards in der Onkologie; 2004:2–172.
- Antoch G, Kuehl H, Kanja J, et al. Dual-modality PET/CT scanning with negative oral contrast agent to avoid artifacts: introduction and evaluation. *Radiology*. 2004;230:879–885.
- Beyer T, Antoch G, Blodgett T, Freudenberg LF, Akhurst T, Mueller S. Dual-modality PET/CT imaging: the effect of respiratory motion on combined image quality in clinical oncology. *Eur J Nucl Med Mol Imaging*. 2003;30:588–596.
- Kumar R, Loving VA, Chauhan A, Zhuang H, Mitchell S, Alavi A. Potential of dual-time-point imaging to improve breast cancer diagnosis with ¹⁸F-FDG PET. *J Nucl Med*. 2005;46:1819–1824.
- Tardivon AA, Athanasiou A, Thibault F, El Khoury C. Breast imaging and reporting data system (BIRADS): magnetic resonance imaging. *Eur J Radiol*. 2007;61:212–215.
- Degani H, Gusis V, Weinstein D, Fields S, Strano S. Mapping pathophysiological features of breast tumors by MRI at high spatial resolution. *Nat Med*. 1997;3:780–782.
- Furman-Haran E, Grobgeld D, Margalit R, Degani H. Response of MCF7 human breast cancer to tamoxifen: evaluation by the three-time-point, contrast-enhanced magnetic resonance imaging method. *Clin Cancer Res*. 1998;4:2299–2304.
- Hauth EA, Jaeger H, Maderwald S, et al. Evaluation of quantitative parametric analysis for characterization of breast lesions in contrast-enhanced MR mammography. *Eur Radiol*. 2006;16:2834–2841.
- Hauth EA, Stockamp C, Maderwald S, et al. Evaluation of the three-time-point method for diagnosis of breast lesions in contrast-enhanced MR mammography. *Clin Imaging*. 2006;30:160–165.
- Beggs AD, Hain SF, Curran KM, O'Doherty MJ. FDG-PET as a “metabolic biopsy” tool in non-lung lesions with indeterminate biopsy. *Eur J Nucl Med Mol Imaging*. 2002;29:542–546.
- Li D, Chen JH, Wang J, Ling R, Yao Q, Wang L. Value of fused ¹⁸F-FDG PET/CT images in predicting efficacy of neoadjuvant chemotherapy on breast cancer [in Chinese]. *Ai Zheng*. 2007;26:900–904.
- Reddy DH, Mendelson EB. Incorporating new imaging models in breast cancer management. *Curr Treat Options Oncol*. 2005;6:135–145.
- Avril N, Rose CA, Schelling M, et al. Breast imaging with positron emission tomography and fluorine-18 fluorodeoxyglucose: use and limitations. *J Clin Oncol*. 2000;18:3495–3502.
- Boone JM, Kwan AL, Yang K, Burkett GW, Lindfors KK, Nelson TR. Computed tomography for imaging the breast. *J Mammary Gland Biol Neoplasia*. 2006;11:103–111.
- Mavi A, Urhan M, Yu JQ, et al. Dual time point ¹⁸F-FDG PET imaging detects breast cancer with high sensitivity and correlates well with histologic subtypes. *J Nucl Med*. 2006;47:1440–1446.
- Fischer U, Kopka L, Grabbe E. Breast carcinoma: effect of preoperative contrast-enhanced MR imaging on the therapeutic approach. *Radiology*. 1999;213:881–888.
- Malich A, Fischer DR, Wurdinger S, et al. Potential MRI interpretation model: differentiation of benign from malignant breast masses. *AJR*. 2005;185:964–970.
- Lehman CD, Blume JD, Weatherall P, et al. Screening women at high risk for breast cancer with mammography and magnetic resonance imaging. *Cancer*. 2005;103:1898–1905.
- Friedrich M. MRI of the breast: state of the art. *Eur Radiol*. 1998;8:707–725.
- Avril N, Schelling M, Dose J, Weber WA, Schwaiger M. Utility of PET in breast cancer. *Clin Positron Imaging*. 1999;2:261–271.
- Wang YYJ, Liu J, Tong Z, Sun X, Yang G. PET-CT in the diagnosis of both primary breast cancer and axillary lymph node metastasis: initial experience. *Int J Radiat Oncol Biol Phys*. 2003;57:362–363.
- Yang WT, Le-Petross HT, Macapinlac H, et al. Inflammatory breast cancer: PET/CT, MRI, mammography, and sonography findings. *Breast Cancer Res Treat*. 2008;109:417–426.